Theoretical Study on the Dehydrogenation Reaction of Alkanes Catalyzed by Zeolites Containing Nonframework Gallium Species

Marcio Soares Pereira and Marco Antonio Chaer Nascimento*

Instituto de Química, Departamento de Físico-Química, Universidade Federal do Rio de Janeiro, Cidade Universitária, CT, Bloco A, sala 412, Rio de Janeiro RJ 21949-900, Brazil

Received: September 9, 2005; In Final Form: December 22, 2005

The dehydrogenation reaction of light alkanes in gallium-containing zeolites was studied by using density functional theory (DFT) and a nonframework gallium species in the dihydridegallium ion form. Two different mechanisms were considered: a 3-step mechanism and a 1-step concerted mechanism. The reactions occurring through the 3-step mechanism showed smaller activation barriers than the ones following the concerted mechanism. However, the energy barrier for the 3-step mechanism seems to be more influenced by the size and type (linear or branched) of the hydrocarbon chain and demands major conformational rearrangement, which could be hampered by the zeolite framework, especially for larger and/or branched hydrocarbons. On the other hand, the concerted mechanism seems to be much less dependent on the substrates geometry. Therefore, the concerted mechanism could be preferential when dealing with larger and/or branched alkanes.

Introduction

The catalytic reforming of naphthas to produce aromatic hydrocarbons, namely benzene, toluene, and xylenes (BTX), is a widely practiced and industrially important technology.[1] While this technology is based on the conversion of C6+ paraffins into aromatics, the use of lower-cost liquefied petroleum gas (LPG), mainly propane and butane, in a dehydrocyclodimerization process with the use of zeolites, in particular with zeolites containing gallium, provides a new and attractive way of producing BTX aromatics. The main difference between reforming and dehydrocyclodimerization, besides the type of catalyst used, is that, in the first process, the molecules are just dehydrogenated and cyclized into aromatics with no mechanism for chain lengthening.[1]

The inclusion of metallic species, such as gallium and zinc, in the zeolite structures, enhances the activity and selectivity toward aromatics products, as reported by several authors.[2−7] The use of gallium seems to be preferable for industrial applications because of the higher stability under operating conditions. For instance, the conversion of propane, in the Cyclar process, jointly developed by British Petroleum and U. O. P., uses a gallium-containing MFI zeolite and produces by weight 63.1% of BTX and 5.9% of molecular hydrogen besides light alkanes, especially ethane and methane.[8,9]

Despite the importance and usefulness of these gallium-containing zeolites and of the process of dehydrocyclodimerization itself, little is known about the mechanisms involved in these reactions and the nature of the active sites. Different gallium incorporation methods can lead to framework or nonframework (and possibly both) gallium species. The first is clearly characterized as substituting isomorphically the aluminum atoms in the original zeolite framework, while the second is still a matter of debate in the literature. Some authors have suggested that the nonframework species are in a gallilic ion form exchanged with the protons of the Brønsted sites in the zeolite,[10] while others have suggested that these species are actually in a dihydride form,[11,12] although also exchanged in the acid sites.

* Corresponding author. E-mail: chaer@iq.ufrj.br.

It is in this perspective that theoretical methods can give the best assistance by proposing mechanisms and models for the catalytic process. Some efforts have already been made in this direction, in particular the study of dehydrogenation of light alkanes with the framework[13] and nonframework[14,15] gallium species, which constitutes the first step in the transformation of light paraffins into BTX aromatics via the dehydrocyclodimerization process.

Recent reports on the dehydrogenation and cracking reactions of light alkanes on zeolites containing framework gallium species indicate that there is little difference in the catalytic behavior between framework gallium and aluminum species. Both the geometries and the activation energies of the transition states are very similar, implying that the framework gallium alone should not be the species responsible for the catalytic enhancement exhibited by gallium-containing zeolites.[13] Therefore, the nonframework gallium species should play a significant role in the dehydrocyclodimerization process involving gallium-containing zeolites. Van Santen et al.[14] studied the dehydrogenation reaction of ethane by using both forms of the nonframework gallium species proposed in the literature. They examined two different mechanisms for each form of gallium, dihydride and gallilic ion, and concluded that the preferable reaction route involved a three-step mechanism and the dihydride form.

In this paper, we examine the mechanism of the dehydrogenation reaction of light paraffins by using a nonframework gallium species model, as proposed by van Santen et al. In this multistep mechanism, the elimination of molecular hydrogen and of the olefin occurs in different steps. Alternatively, we propose a new concerted mechanism in which both the elimination of olefin and of molecular hydrogen occur in the same step. We also present a discussion of the different characteristics of both mechanisms. A preliminary investigation of the different mechanisms for the ethane reaction has been published elsewhere.[16]

Models and Computational Details

All reactions were studied by using a T5 cluster with gallium dihydride to model the nonframework gallium (Figure 1). A

10.1021/jp055104g CCC: $33.50
Published on Web 01/28/2006

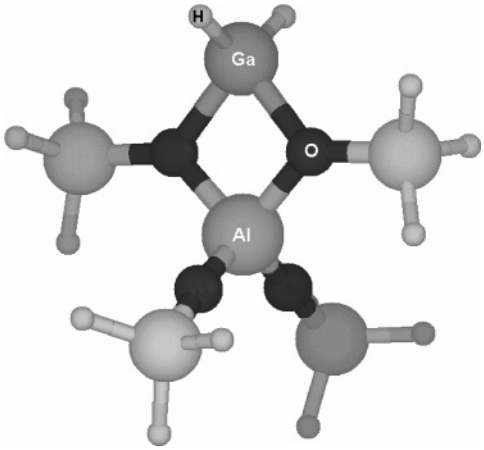

Figure 1. T5 cluster with nonframework gallium in dihydride ion form.

similar cluster (T5) was used in previous studies to model the zeolite framework.[13,17−19] We are quite aware of the limitations of this cluster model. Indeed, several approaches using embedding techniques,[20,21] periodic DFT calculations,[22,23] and different ONIOM[24,25] schemes have been described in the literature. The embedding technique corrects the activation energy for the influence of the cavity but does not allow for changes either in the spatial distribution of the substrates or in the geometry of the TS in response to the presence of the cavity. The periodic calculations demand high computational power, and only zeolites with small unit cells can be effectively studied. The QM/MM methods represent a computationally cheaper alternative, but the final results may be quite dependent on the choice of the QM/MM borderline and on the level of calculation employed for the MM part of the system. Therefore, the cluster approach still represents a very convenient procedure for theoretical studies on the catalytic behavior of zeolites of chemical interest, such as HZSM-5, HY, USY, etc. In particular, as shown in other publications, at least for small sized substrates, the use of larger clusters do not introduce any changes in the mechanism but only in the energetic of the reactions.[26,27] Therefore, the mechanism of the reaction, as well as the relative energies, can be well established with the T5 model.

Density functional theory (DFT) with the B3LYP[28,29] hybrid exchange-correlation functional was used to perform all the calculations. Geometry optimization and saddle point searches were all performed by using the program JAGUAR version 4.2[30] with the LACVP basis set (6-31G** and effective core potential (ECP) for Ga) and JAGUAR version 5.5[31] with the LACV3P basis set (6-311G** and effective core potential (ECP) for Ga). The intrinsic reaction coordinate (IRC)[32] calculations were performed with GAUSSIAN 98.[33] A DFT method was chosen because very reasonable results can be obtained at relatively low computational costs. The B3LYP functional has been largely used in other calculations,[16−19] including some with gallium atoms,[13,14] providing, among the presently available functionals, the best description of these reactions. The LACVP basis set has already been used in a previous work,[13] and the use of the ECP caused an increase no greater than 2 kcal/mol in the computed energies, which is less than the limit of accuracy of the present level of theory. At the level of calculation employed, basis set superposition errors are of the order of 0.7 kcal/mol.[19]

No restrictions were imposed during geometry optimization, IRC, and saddle point searches. No attempts have been made at calculating adsorption energies because, in the present case, they should be dominated by weak interactions such as dispersion forces, which are poorly described by the presently available DFT functionals, although the newly proposed X3LYP functional[34] may minimize this problem.

SCHEME 1: Ethane Dehydrogenation Reaction through the 3-Step Mechanism with the 6-311G Basis Sets**

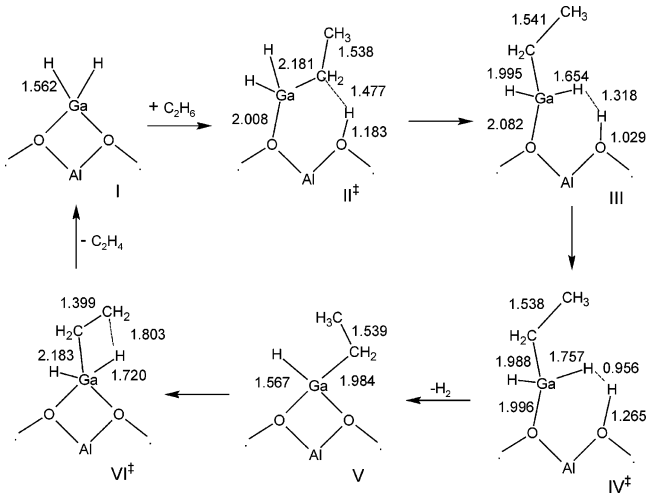

Results and Discussion

The dehydrogenation reaction of light paraffins by a gallium-containing ZSM-5 zeolite was studied by using a T5 cluster as a model for the zeolite and the dihydridegallium ion as the gallium species, as originally proposed by Meitzner et al.[11] The dehydrogenation reaction of ethane, propane, butane, and isobutane were studied and two different mechanisms examined. The reactions were studied by using both 6-31G** and 6-311G** basis sets to verify the influence of the basis set on the results. The calculated total energies and imaginary frequencies (reaction coordinates) for the structures involved in each reaction are shown in Tables 1 and 2.

The dihydridegallium species has been used before by van Santen et al.[14] to model the dehydrogenation of ethane to ethene in a gallium-containing zeolite. According to the calculations, this reaction proceeds through a 3-step mechanism, including the regeneration of the dihydride gallium species in the active site. However, they used a T3 model for the active site and a different basis set. Thus, to compare the 3-step mechanism with the concerted one, we also examined the former mechanism with the T5 model and with the same basis set used in the calculations performed for the concerted mechanism. As expected, the reaction profile, geometrical parameters, and energies of the transition states and intermediates vary slightly with the basis set.

The 3-step reaction for the dehydrogenation of ethane proceeds as displayed in Scheme 1. In the first step, a carbon−hydrogen bond is broken with the simultaneous formation of a bond between the positively charged gallium atom and the negatively charged alkyl group. A bond between the oxygen of the zeolite site and the proton released by the ethane molecule is also formed, creating a zeolitic Brønsted acid site. A rotation along the Ga−O axis leads to structure III, which already displays a strong interaction between the proton of the Brønsted site and the dihydride site.

In the second step, molecular hydrogen is eliminated by the combination of the proton of the Brønsted site and the hydride ion from the gallium site. It is interesting noting that the transition state IV‡and the intermediate III have very similar geometries, the only significant difference being the position of the hydride ion and the proton. As expected, in the transition

TABLE 1: Energy (B3LYP/6-31G and B3LYP/6-311G** with ZPE Correction) for the Transition States and Intermediates of the Dehydrogenation Reaction through the 3-step Mechanism and the Reaction Coordinates (Imaginary Frequency: IF)**

	6-31G**		6-311G**	
ethane	*E* (hartree)	IF (cm^{-1})	*E* (hartree)	IF (cm^{-1})
II‡	−1791.743684	−1007.60	−1791.998607	−1015.55
IV‡	−1791.756763	−640.61	−1792.011562	−615.21
VI‡	−1791.712582	−660.25	−1791.969679	−710.45
I (*cluster* T5)	−1712.052401		−1712.289026	
III	−1791.759666		−1792.012983	
V	−1791.804428		−1792.057900	

	6-31G**		6-311G**			6-31G**		6-311G**	
propane	*E* (hartree)	IF (cm^{-1})	*E* (hartree)	IF (cm^{-1})	propane-2 [a]	*E* (hartree)	IF (cm^{-1})	*E* (hartree)	IF (cm^{-1})
II‡	−1831.033571	−1017.16	−1831.295158	−1032.60	II‡	−1831.024929	817.21	−1831.286610	−850.27
IV‡	−1831.044955	−593.23	−1831.307955	−574.18	IV‡	−1831.041226	645.43	−1831.304810	−587.52
VI‡	−1831.007547	−650.97	−1831.273515	−702.15	VI‡	−1831.001036	756.41	−1831.264445	−768.98
I (*cluster* T5)	−1712.052401		−1712.289026		I (*cluster* T5)	−1712.052401		−1712.289026	
III	−1831.045904		−1831.309521		III	−1831.043536		−1831.306162	
V	−1831.090323		−1831.354412		V	−1831.088390		−1831.350270	

	6-31G**		6-311G**			6-31G**		6-311G**	
butane	*E* (hartree)	IF (cm^{-1})	*E* (hartree)	IF (cm^{-1})	butane-2 [a]	*E* (hartree)	IF (cm^{-1})	*E* (hartree)	IF (cm^{-1})
II‡	−1870.320378	−1002.65	−1870.591322	−1035.22	II‡	−1870.311096	−828.89	−1870.581451	−828.61
IV‡	−1870.331911	−668.45	−1870.604028	−575.12	IV‡	−1870.327361	−600.00	−1870.599017	−582.30
VI‡	−1870.297205	−671.70	−1870.569706	−677.32	VI‡	−1870.286058	−733.64	−1870.565957	−759.99
I (*cluster* T5)	−1712.052401		−1712.289026		I (*cluster* T5)	−1712.052401		−1712.289026	
III	−1870.334261		−1870.605537		III	−1870.329293		−1870.600526	
V	−1870.379829		−1870.650437		V	−1870.374702		−1870.645043	

	6-31G**		6-311G**			6-31G**		6-311G**	
isobutane	*E* (hartree)	IF (cm^{-1})	*E* (hartree)	IF (cm^{-1})	isobutane-2 [a]	*E* (hartree)	IF (cm^{-1})	*E* (hartree)	IF (cm^{-1})
II‡	−1870.320394	−1018.97	−1870.590401	−1012.27	II‡	−1870.302683	−1003.32	−1870.572968	−1037.81
IV‡	−1870.332980	−648.41	−1870.604749	−623.06	IV‡	−1870.328088	−577.61	−1870.600216	−574.18
VI‡	−1870.301722	−667.76	−1870.57552	−707.11	VI‡	−1870.287690	−795.01	−1870.559547	−702.15
I (*cluster* T5)	−1712.052401		−1712.289026		I (*cluster* T5)	−1712.052401		−1712.289026	
III	−1870.333810		−1870.606154		III	−1870.329281		−1870.600714	
V	−1870.378487		−1870.649851		V	−1870.374613		−1870.645364	
V	−1870.378487		−1870.649851		V	−1870.374613		−1870.645364	

[a] Dehydrogenation reaction through the second channel

TABLE 2: Energy (B3LYP/6-31G and B3LYP/6-311G** with ZPE Correction) of the Structures Involved in the Dehydrogenation Reaction through the Concerted Mechanism and the Reaction Coordinates (Imaginary Frequency: IF)**

	6-31G**		6-311G**	
structure	*E* (hartree)	IF (cm^{-1})	*E* (hartree)	IF (cm^{-1})
ethane	−1791.710351	−1097.04	−1791.966304	−1086.54
propane	−1830.999923	−1100.72	−1831.264600	−1123.53
butane	−1870.288368	−1104.71	−1870.560166	−1116.07
butane-2	−1870.290664	−1115.52	−1870.562306	−1114.57
isobutane	−1870.288917	−1124.94	−1870.563971	−1130.95
T5 *cluster*	−1712.052401		−1712.289026	
ethane	−79.763804		−79.781843	
propane	−119.051612		−119.077631	
butane	−158.339612		−158.373491	
isobutane	−158.340887		−158.374887	

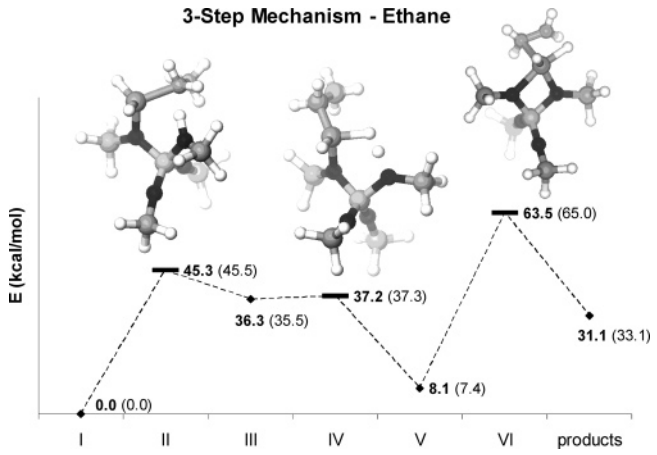

Figure 2. Ethane dehydrogenation pathway through the 3-step mechanism with 6-311G** and ECP for the Ga atom. Values in parentheses for the 6-31G** basis set and ECP for Ga.

state IV‡ (Scheme 1), the distance between the hydride and the proton is smaller. The activation energy of this step is also particularly small (∼1 kcal/mol), as can be seen in Figure 2. In fact, this energy is smaller than the accuracy that can be expected from the DFT functional used in the calculation. To investigate possible failures of the DFT method in the description of this particular step of the reaction, the reactants and the TS were re-optimized at the MP2 level by using the 6-311G** basis set. At this level of calculation, the barrier is of 7.6 kcal/mol, again much smaller than those of the other steps of the reaction. Thus, the fact that this step of the reaction may not be properly described either at the DFT/B3LYP or MP2 levels does not change the analysis of the reaction pathway.

SCHEME 2: Propane Dehydrogenation Reaction through the 3-step Mechanism (First Channel) with the 6-311G**

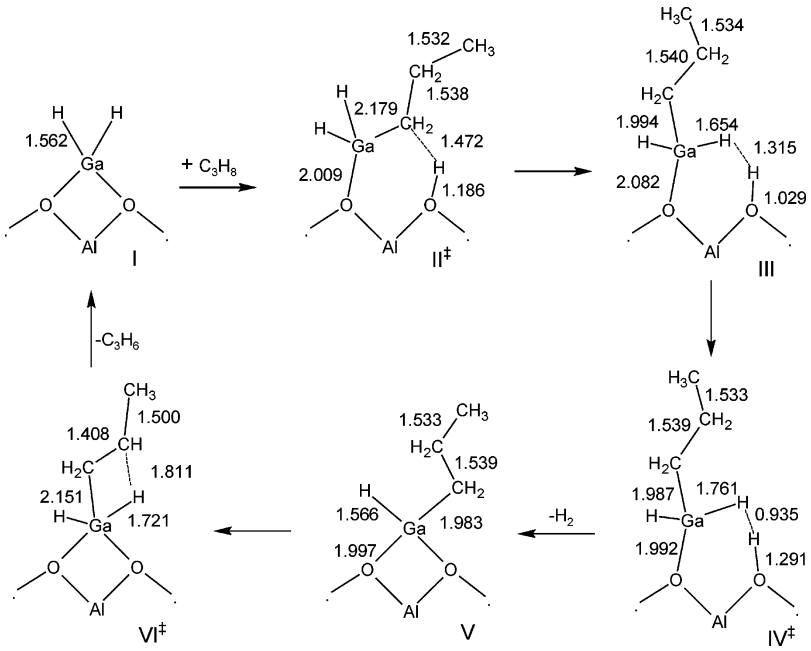

In the last step, the olefin elimination with the regeneration of the catalytic site, there is a reorientation of the alkyl fragment such that both carbon atoms, the gallium atom and the hydrogen atom bound to the β-carbon (the one connected to the carbon bound to the gallium atom) become aligned in the same plane, with a dihedral angle near zero. This β-hydrogen atom is then transferred to the gallium atom with the simultaneous cleavage of the gallium−carbon bond, eliminating ethene and regenerating the catalytic site.

According to the reaction coordinate in Figure 2, it is clear that the elimination of ethene in the last step, with an activation energy of 55 kcal/mol, controls the reaction rate. The breaking of the C−H bond of ethane, in the first step, also presents a high energy barrier, while the elimination of molecular hydrogen, in the second step, proceeds smoothly with an activation energy of ∼1 kcal/mol. As mentioned before, even if not properly described, this barrier is much smaller than those of the other steps of the reaction, and therefore, this result does not change the analysis of the reaction pathway.

The propane dehydrogenation reaction was also investigated and two different reaction channels were examined. The first channel involves, in the first step of the reaction, the breaking of a primary carbon−hydrogen bond, while in the second channel, the carbon−hydrogen bond broken in the first step is that of the secondary carbon. In the first channel, the same 3-step mechanism was observed, as displayed in Scheme 2. The mechanism, in general, is very similar to the one involving the ethane molecule studied by van Santen et al.,[14] but with some minor differences.

In the first step, the geometry of both the intermediate III and transition state II‡ are very similar to that of the respective ones in the reaction with ethane. The activation energy of this step is almost the same as that of the reaction for the ethane molecule as well.

In the molecular hydrogen elimination step, the intermediate again closely resembles that of the previously described reaction with ethane, while, in the transition state IV‡, the proton from the Brønsted site and the hydride from the gallium site are slightly closer to each other and both slightly more separated from the rest of the cluster.

In the last step, olefin elimination, the transition state VI‡ also resembles the corresponding one for the ethane reaction. In this transition state, the four atoms involved in bond formation and bond cleavage are arranged in a plane, just as in the previous case of the ethane reaction. The bond lengths, nevertheless, are slightly different from the previous case. The Ga−C bond is shorter, while the Ga−O, C−C, and C−H distances are slightly larger when compared to the case of ethane. As a result, the distance between the propyl fragment and the "Z⁻" cluster modeling the zeolite is larger. The activation energy for this step is 4.6 kcal/mol smaller (Figure 3) when compared to the dehydrogenation reaction of ethane.

The reaction through the second channel follows a mechanism very similar to the one of the reaction of butane through the second channel (as discussed below).

The butane dehydrogenation reaction was also investigated through two different reaction channels. The first channel involves, in the first step of the reaction, the breaking of a carbon−hydrogen bond of a primary carbon, which leads to a 1-butene product. Through the second channel, the carbon−

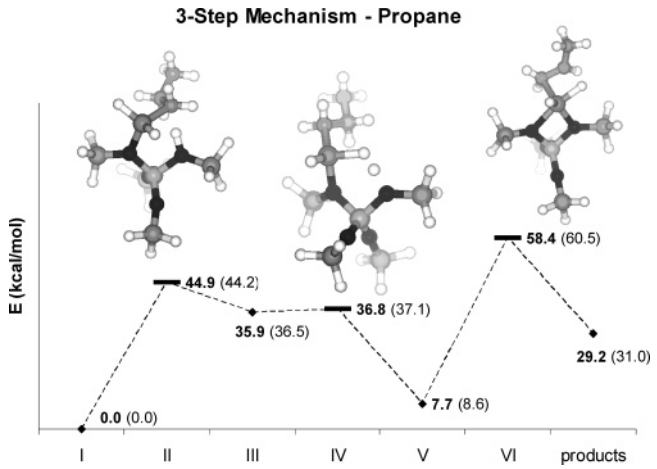

Figure 3. Propane dehydrogenation pathway through the 3-step mechanism (first channel) with 6-311G** and ECP for the Ga atom. Values in parentheses for the 6-31G** basis and ECP for the Ga atom.

SCHEME 3: Butane Dehydrogenation Reaction through the 3-step Mechanism (Second Channel) with the 6-311G**

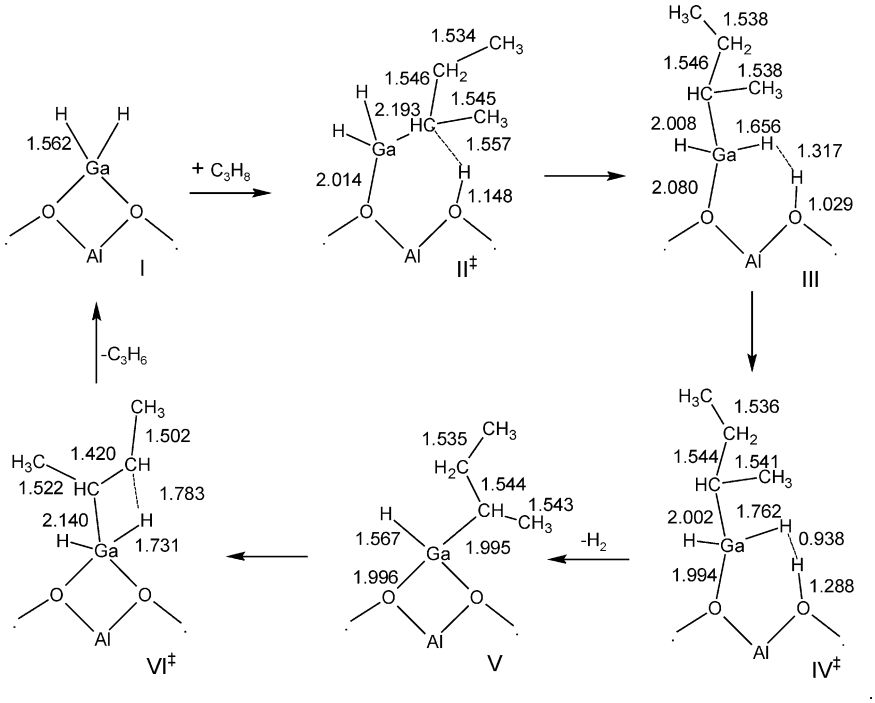

hydrogen bond broken in the first step is that of the secondary carbon, leading to the formation of 2-butene.

The reaction of butane through the first channel closely resembles the reaction with propane through the first channel if one considers both the geometric parameters and the energies. The reaction through the second channel also resembles the reaction with propane (through the second channel) and can be seen in Scheme 3.

In the first step, the C−H and C−Ga distances of the transition state are larger than in the previous cases, while the O−H bond is smaller. These differences account for a further separation between the alkyl fragment and the zeolite framework, most likely due to a steric effect. The activation energy for this step is 6 kcal/mol higher (Figure 4) than the respective one through the first channel of the butane dehydrogenation reaction.

The second step proceeds as in the case of propane with a slightly larger Ga−C distance. The activation energy, nevertheless, is still negligible.

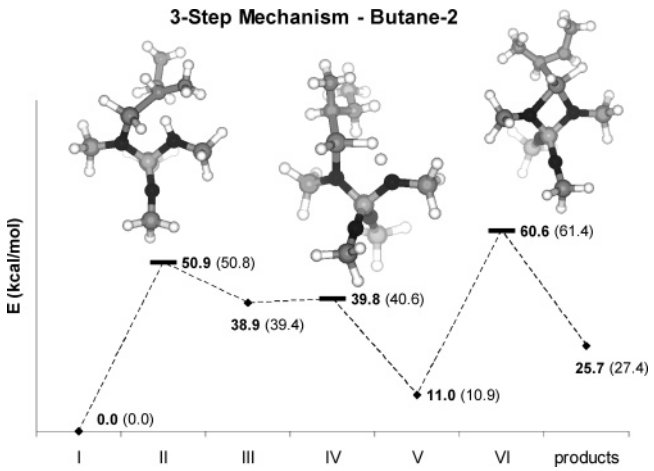

Figure 4. Butane dehydrogenation pathway through the 3-step mechanism (second channel) with 6-311G** and ECP for the Ga atom. Values in parentheses for the 6-31G** basis and ECP for the Ga atom.

In the last step, the geometric parameters of the transition state change, when compared to the previous cases, to further separate the alkyl fragment from the zeolite framework. The activation barrier of this step is 6 kcal/mol smaller than the corresponding one in the reaction of butane through the first channel.

This decrease in the activation energy of the last step of the reaction, together with the increase in the activation energy for the first step, may induce a change in the mechanism of this reaction when compared to the case of ethane. While in the previous cases, the reaction seem clearly controlled by the olefin elimination step, in the butane reaction through the second channel, the activation energy for the C−H bond-breaking step is slightly higher (∼1 kcal/mol) than that of the olefin elimination step.

The isobutane dehydrogenation reaction was also investigated through two different channels. The first channel involves the breaking of a primary carbon−hydrogen bond, while the second channel involves the breaking of the tertiary carbon−hydrogen bond in the first step of the reaction. Both channels lead to isobutene as the product.

The reaction of dehydrogenation of isobutane through the first channel is similar to the reactions of propane and butane through the same channel. The main difference among those reactions and the reaction with isobutane resides in the third step, where the distance between the isobutyl fragment and the zeolite framework is larger than the corresponding distance in the propane and butane reactions. The activation barrier for this step is also 4 kcal/mol smaller than the barrier for the reaction with butane.

The reaction through the second channel is markedly different from the one through the first channel. In the first step, the C−H and Ga−C distances of the transition state are significantly larger, as displayed in Scheme 4. The activation energy for the first step is 11 kcal/mol higher (Figure 5) than that of the reaction through the first channel.

The second step resembles that of the previous cases, again with a very small activation energy (1.3 kcal/mol). However,

SCHEME 4: Isobutane Dehydrogenation Reaction through the 3-step Mechanism (Second Channel) with the 6-311G**

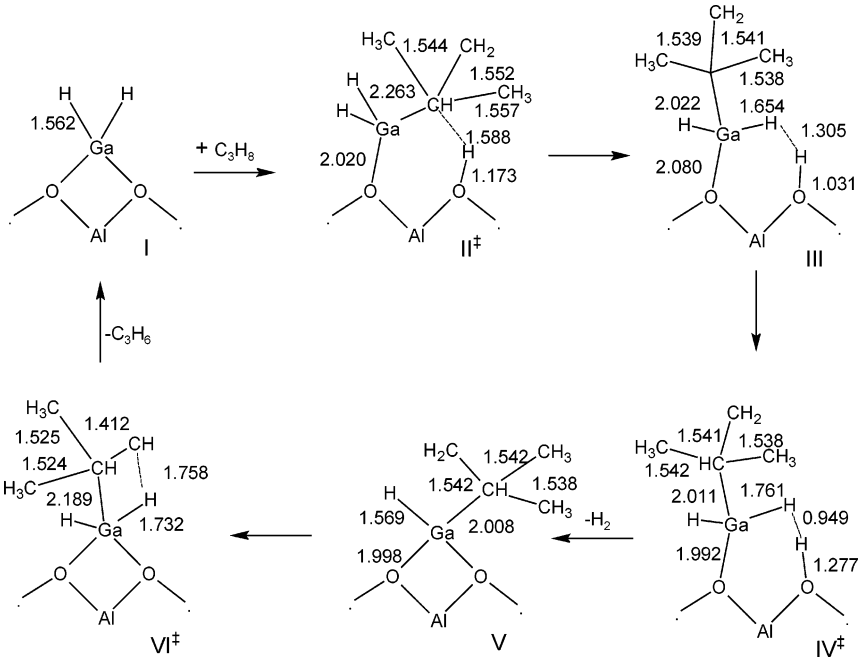

TABLE 3: Activation Energies (kcal/mol) for the Dehydrogenation Reaction through the 3-Step and the Concerted Mechanisms

			3-Step					
	concerted		6-31G**			6-311G**		
structure	6-31G**	6-311G**	first step	second step	third step	first step	second step	third step
ethane	66.4	65.5	45.5	1.8	57.6	45.4	0.9	55.4
propane	65.3	64.0	44.2	0.6	51.9	44.9	1.0	50.8
propane-2[a]			49.6	1.5	54.8	50.2	0.9	53.9
butane	65.0	64.2	45.0	1.5	51.8	44.7	0.9	50.7
butane-2[a]	63.6	62.9	50.8	1.2	50.5	50.9	1.0	49.6
isobutane	65.5	62.7	45.7	0.5	48.2	46.1	0.9	46.6
isobutane-2[a]			56.9	0.7	54.5	57.1	0.3	53.9

[a] Dehydrogenation reaction through the second channel.

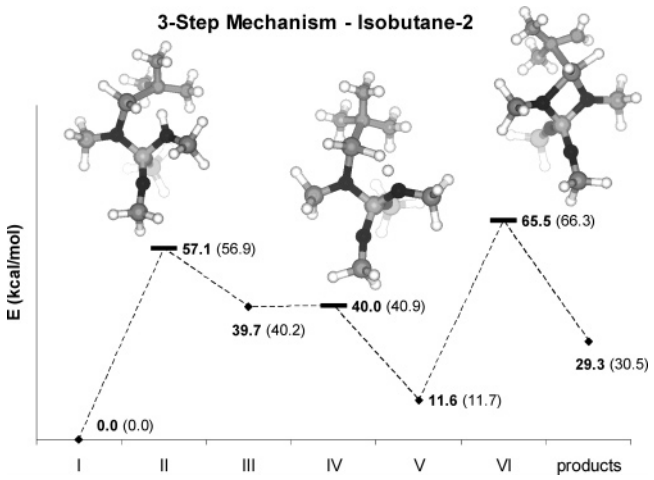

Figure 5. Isobutane dehydrogenation pathway through the 3-step mechanism (second channel) with 6-311G** and ECP for the Ga atom. Values in parentheses for the 6-31G** basis and ECP for the Ga atom.

as discussed before, the fact that this step may not be properly described at the B3LYP level does not change the analysis about the reaction pathway.

In the third step, the Ga−C and C−CH_3 distances are larger than in the reaction through the first channel, while the C−H distance is smaller. The activation energy is 7 kcal/mol higher than the corresponding one in the reaction of isobutane through the first channel.

In this case, as with the previous case of the dehydrogenation reaction of butane through the second channel, there could be a change in the mechanism because the activation barrier of the first step is slightly higher (∼3 kcal/mol) than that of the olefin elimination step.

Thus, according to the 3-step mechanism, all dehydrogenation reactions of light paraffins should proceed through the primary carbon, especially as one increases the hydrocarbon chain and uses more branched alkanes. Otherwise, if the reaction proceeds through a secondary or tertiary carbon, the first step of the reaction, the H−C bond breaking, becomes less favorable, while the elimination of the formed olefin in the last step becomes more favorable. This could lead to a change in the mechanism of these reactions. However, because of the small difference in energy, this change in the mechanism must be confirmed with a higher-level calculation.

The dehydrogenation reaction of these light paraffins was also investigated by assuming that the H−C bond cleavage and both molecular hydrogen and olefin elimination occur simultaneously in a one-step concerted mechanism. The transition states of the reactions with ethane, propane, butane, and isobutane, according to this mechanism, are displayed in Scheme 5.

All the transition states involved in the dehydrogenation reaction through the concerted mechanism, despite the basis employed, are similar in geometry, with some minor differences in bond lengths, as shown in Scheme 5. Although there are some differences in the geometric parameters among these transition

SCHEME 5: Transition States for the Dehydrogenation Reactions through the Concerted Mechanism with the 6-311G**

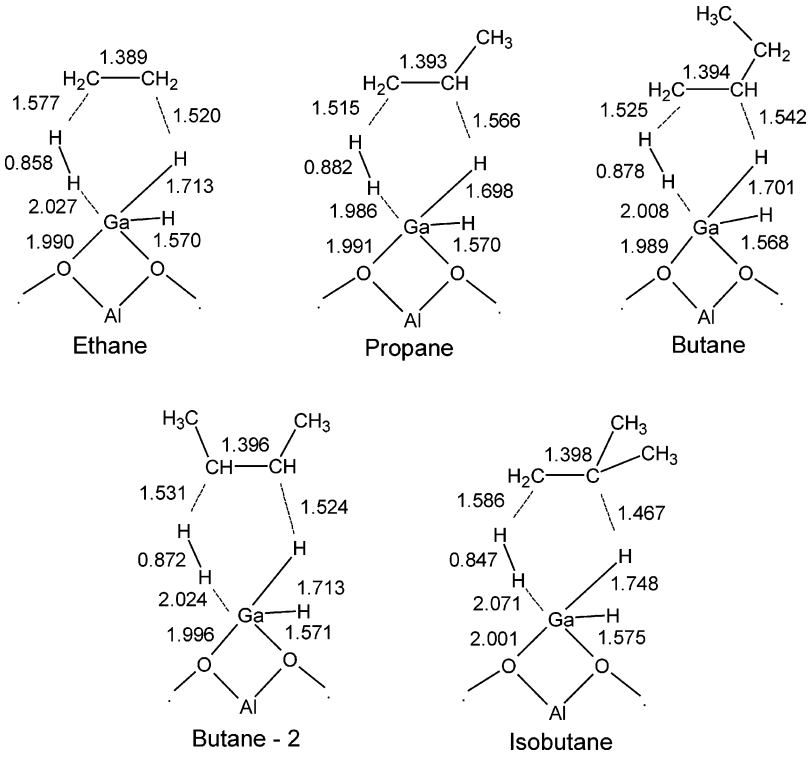

states, the activation energies for these reactions are almost the same, as displayed in Table 3. This behavior indicates that these transition states are less dependent on the geometry of the reactants than the transition states in the 3-step mechanism. From Scheme 5, it can be seen that, as the size of the alkane increases, there is a slight change in the geometry to reduce the interaction between the extra methyl groups and the zeolite framework. Nevertheless, the activation energies remain practically unchanged.

To achieve a better understanding of the concerted mechanism, an intrinsic reaction coordinate (IRC) calculation was performed for the dehydrogenation of ethane (Figure 6). The atomic charges were calculated from the electrostatic potential (ESP), with the CHELG algorithm at each step, and are summarized in Figure 6b. From Figure 6a, one sees that, as the H2−Ga and C1−H3 bonds are broken, hydrogen H4 is transferred to the gallium site and molecular hydrogen is formed from species H2 and H3. From Figure 6b, one sees that, as the reaction proceeds, the charge distribution among the atoms is such as to form the neutral products, molecular hydrogen and olefin, while simultaneously reconstructing the catalytic site.

Conclusions

The dehydrogenation reactions of light alkanes catalyzed by gallium-exchange zeolites was investigated at the B3LYP/6-31G** and B3LYP/6-311G** levels of calculation. Two distinct mechanisms were considered: the 3-step mechanism, as proposed by van Santen et al.[14] and a concerted mechanism.

The 3-step reaction presents an activation energy of approximately 10−15 kcal/mol smaller than the corresponding activation energies in the concerted mechanism. However, the 3-step mechanism requires major conformational rearrangements between steps, which could be hampered by the zeolite framework in the case of large or more branched substrates. Furthermore, the activation energies of the first and last steps in the 3-step mechanism are somewhat more sensitive to the substrate geometry than the activation energy of the concerted mechanism. This could favor the concerted mechanism if the effect of the zeolite cavity was considered, although further calculation incorporating these effects should be employed in order to verify this assumption. The concerted mechanism, on the other hand, is simpler when compared to the 3-step

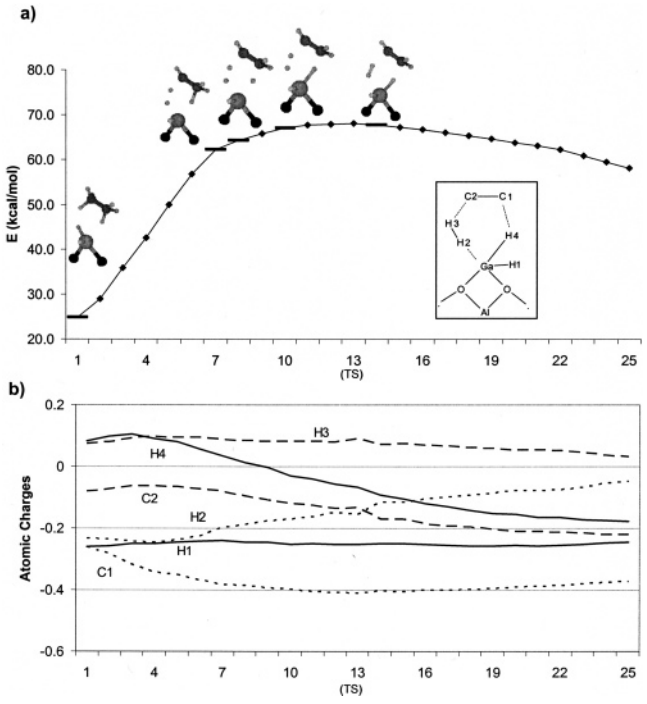

Figure 6. IRC calculation for the ethane dehydrogenation reaction through the concerted mechanism. (a) Structural and energy changes along the reaction coordinate; (b) atomic charges along the reaction coordinate.

mechanism. No conformational rearrangements are necessary and the reaction proceeds in a unique step, as opposed to the 3-step mechanism, for which two of the steps require activation barriers of the same order.

Extraframework gallium species are certainly connected to the enhancement observed in dehydrocyclodimerization processes catalyzed by gallium-containing zeolites. The dehydride-gallium ion model for these nonframework species seems to be able to describe the dehydrogenation reactions involved in this aromatization process through two different mechanisms. These different mechanisms could be responsible for different dehydrogenation steps in the aromatization process.

Acknowledgment. We thank CAPES, CNPq, FAPERJ, PRONEX, and Instituto do Milênio de Materiais Complexos for financial support.

References and Notes

(1) Seddon, D. *Catal. Today* **1990**, *6*, 351.
(2) Brabec, L.; Jeschke, M.; Meusinger, J. *Appl. Catal., A* **1998**, *167*, 309.
(3) Price, G. L.; Kanazirev, V.; Dooley, K. M.; Hart, V. I. *J. Catal.* **1998**, *173*, 12.
(4) Bayense, C. R.; van der Pol, A. J. H. P.; van Hoof, J. H. C. *Appl. Catal.* **1991**, *72*, 81.
(5) Gianetto, G.; Montes, A.; Gnep, N. S.; Guisnet, M. *J. Catal.* **1993**, *145*, 86.
(6) Inui, T,; Nagata, H.; Matsuda, H.; Kim, J.-B.; Ishihara Y. *Ind. Eng. Chem. Res.* **1992**, *31*, 995.
(7) Gnep, N. S.; Doyemet, J. Y.; Seco, A. M.; Ribeiro F. R.; Guisnet, M. *Appl. Catal.* **1988**, *43*, 155.
(8) Mowry, J. R.; Anders, R. E.; Johson, J. A. *Oil Gas J.* **1985**, *83*, 128.
(9) Mowry, J. R.; Martindale, D. C.; Hall, P. H. *Arabian J. Sci. Eng.* **1985**, *10*, 36.
(10) Dooley, K. M.; Chang, C.; Price, G. L. *Appl. Catal., A* **1992**, *84*, 17.
(11) Meitzner, G. D.; Iglesia, E.; Baumgartner, J. E.; Huang, E. S. *J. Catal.* **1993**, *140*, 209.
(12) Kazansky, V. B.; Subbotina, I. R.; Rane, N.; van Santen R. A.; and Hensen, E. J. M. *Phys. Chem. Chem. Phys.* **2005**, *7*, 3088.
(13) Pereira M. S.; Nascimento, M. A. C. *Theor. Chem. Acc.* **2003**, *110*, 441.
(14) Frash, M. V.; van Santen, R. A. *J. Phys. Chem. A* **2000**, *104*, 2468.
(15) Rosanska, X.; García-Sánchez, M.; Hensen, E. J. M.; van Santen, R. A. *C. R. Acad. Sci., Ser. IIc: Chim.* **2005**, *8*, 509.
(16) Pereira, M. S.; Nascimento, M. A. C. *Chem. Phys. Lett.* **2005**, *406*, *446*.
(17) Furtado, E. A.; Milas, I.; Lins, J. O. M. A.; Nascimento, M. A. C. *Phys. Status Solidi A* **2001**, *187*, 275.
(18) Furtado, E.; Nascimento, M. A. C. In *Theoretical Aspects of Heterogeneous Catalysis*; Kluwer: Dordrecht, 2001; p 39
(19) Milas I.; Nascimento, M. A. C. *Chem. Phys. Lett.* **2001**, *338*, 67.
(20) Sherwood, P.; de Vries A. H.; Collins, S. J.; Greatbanks, S. P.; Burton, N. A.; Vincent, M. A.; Hillier, I. H. *Faraday Disc.* **1997**, *106*, 79.
(21) Martinez-Magadan, J. M.; Cuan, A.; Castro, M. *Int. J. Quant. Chem.* **2002**, *88*, 750.
(22) Rozanska, X.; van Santen, R. A.; Hutschka, F. *J. Phys. Chem. B* **2002**, *106*, 4652.
(23) Rozanska, X.; Demuth, Th.; Hutschka, F.; Hafner, J.; van Santen, R. A. *J. Phys. Chem. B* **2002**, *106*, 3248.
(24) Boronat, M.; Viruela, P. M.; Corma, A. *J. Am. Chem. Soc.* **2004**, *126*, 3300.
(25) Tuma, C.; Sauer, J. *Chem. Phys. Lett.* **2004**, *387*, 388.
(26) Milas I.; Nascimento, M. A. C. *Chem. Phys. Lett.* **2003**, *373*, 379.
(27) Milas I.; Nascimento, M. A. C. *Chem. Phys. Lett.* **2005**, *418*, 364.
(28) Becke, A. D. *J. Chem. Phys.* **1993**, *98*, 5648.
(29) Lee, C.; Yang, W.; Parr, R. G. *Phys. Rev. B* **1988**, *37*, 786.
(30) *Jaguar 4.2*; Schrödinger, Inc.: Portland OR, 1998.
(31) *Jaguar 5.5*; Schrödinger, Inc.: Portland OR, 1998.
(32) Gonzales, C.; Schlegel, H. B. *J. Chem. Phys.* **1989**, *90*, 2154.
(33) Frisch, M. J.; Trucks, G. W.; Schlegel, H. B.; Scuseria, G. E.; Robb, M. A.; Cheeseman, J. R.; Zakrzewski, V. G.; Montgomery, J. A., Jr.; Stratmann, R. E.; Burant, J. C.; Dapprich, S.; Millam, J. M.; Daniels, A. D.; Kudin, K. N.; Strain, M. C.; Farkas, O.; Tomasi, J.; Barone, V.; Cossi, M.; Cammi, R.; Mennucci, B.; Pomelli, C.; Adamo, C.; Clifford, S.; Ochterski, J.; Petersson, G. A.; Ayala, P. Y.; Cui, Q.; Morokuma, K.; Malick, D. K.; Rabuck, A. D.; Raghavachari, K.; Foresman, J. B.; Cioslowski, J.; Ortiz, J. V.; Stefanov, B. B.; Liu, G.; Liashenko, A.; Piskorz, P.; Komaromi, I.; Gomperts, R.; Martin, R. L.; Fox, D. J.; Keith, T.; Al-Laham, M. A.; Peng, C. Y.; Nanayakkara, A.; Gonzalez, C.; Challacombe, M.; Gill, P. M. W.; Johnson, B. G.; Chen, W.; Wong, M. W.; Andres, J. L.; Head-Gordon, M.; Replogle, E. S.; Pople, J. A. *Gaussian 98*, revision A.6; Gaussian, Inc.: Pittsburgh, PA, 1998.
(34) Xu, X.; Zhang, Q.; Muller, R. P.; Goddard, W. A., III. *J. Chem. Phys.* **2005**, *122*, 014105.